THE JOURNAL OF PHYSICAL CHEMISTRY C

Article

pubs.acs.org/JPCC

Atomic Surface Structure of CH_3-Ge(111) Characterized by Helium Atom Diffraction and Density Functional Theory

Zachary M. Hund,[†] Kevin J. Nihill,[†] Davide Campi,[‡] Keith T. Wong,[§] Nathan S. Lewis,[§] M. Bernasconi,[‡] G. Benedek,[‡,∥] and S. J. Sibener*,[†]

[†]The James Franck Institute and Department of Chemistry, The University of Chicago, 929 E. 57th Street, Chicago, Illinois 60637, United States

[‡]Dipartimento di Scienza dei Materiali, Universita di Milano-Bicocca, Via Cozzi 53, 20125 Milano, Italy

[§]Beckman Institute and Kavli Nanoscience Institute, Division of Chemistry and Chemical Engineering, 210 Noyes Laboratory, 127-72, California Institute of Technology, Pasadena, California 91125, United States

[∥]Donostia International Physics Center (DIPC), Universidad del País Vasco (EHU), 20018 Donostia/San Sebastian, Spain

ABSTRACT: The atomic-scale surface structure of methyl-terminated germanium (111) has been characterized by using a combination of helium atom scattering and density functional theory. High-resolution helium diffraction patterns taken along both the $\langle\bar{1}2\bar{1}\rangle$ and the $\langle 01\bar{1}\rangle$ azimuthal directions reveal a hexagonal packing arrangement with a 4.00 ± 0.02 Å lattice constant, indicating a commensurate (1 × 1) methyl termination of the primitive Ge(111) surface. Taking advantage of Bragg and anti-Bragg diffraction conditions, a step height of 3.28 ± 0.02 Å at the surface has been extracted using variable de Broglie wavelength specular scattering; this measurement agrees well with bulk values from CH_3-Ge(111) electronic structure calculations reported herein. Density functional theory showed that methyl termination of the Ge(111) surface induces a mild inward relaxation of 1.66% and 0.60% from bulk values for the first and second Ge−Ge bilayer spacings, respectively. The DFT-calculated rotational activation barrier of a single methyl group about the Ge−C axis on a fixed methyl-terminated Ge(111) surface was found to be approximately 55 meV, as compared to 32 meV for a methyl group on the H-Ge(111) surface, sufficient to hinder the free rotation of the methyl groups on the Ge(111) surface at room temperature. However, accurate MD simulations demonstrate that cooperative motion of neighboring methyl groups allows a fraction of the methyl groups to fully rotate on the picosecond time scale. These experimental data in conjunction with theory provide a quantitative evaluation of the atomic-scale surface structure for this largely unexplored, yet technologically interesting, hybrid organic−semiconductor interface.

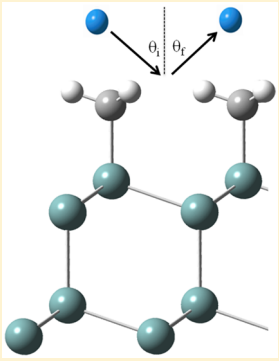

1. INTRODUCTION

High-quality Ge surfaces are desirable for applications in high-speed circuits and the collection of infrared radiation in multijunction solar cells due to their high hole-carrier mobility (4 times that of Si) and 0.67 eV band gap.[1−4] The high surface-state density of the GeO_x/Ge interface and the presence of unstable, water-soluble GeO_2 sites have, however, inhibited the commercial implementation of Ge-based technology.[5,6] Methods that passivate the Ge surface while preventing the formation of an oxide overlayer are, therefore, highly desirable. For example, hydrogenation of the semiconductor surface via chemisorption deconstructs Si(100)-(2 × 1) or Ge(100)-(2 × 1) back to their primitive (1 × 1) structure, creating large, atomically flat terraces of surface atoms passivated by a single layer of hydrogen. Hydrogen-termination of Si(111) and Ge(111) also deconstructs the well-known (7 × 7) and (2 × 8) clean structures for Si and Ge, respectively, and they represent two of the simplest semiconductor surfaces, retaining a bulk-like structure except for mild relaxations of their outermost bilayer spacings. Therefore, these surfaces have attracted considerable interest with respect to elucidating their surface structure through both theory and experiment.[7−14]

Hydrogen passivation of Ge does not provide the same long-term protection against oxidation and reconstruction as seen with H-Si.[15,16] As with Si, the high quality and functionality of the hydrogen-terminated Ge surface can be used as a platform for grafting 1-alkenes to the H-Ge(111) surface to form a stable C−Ge bond.[17−21] Alkylation of the Ge surface has proven to be a robust method for creating densely packed, long-chain alkyl layers that add resistance to oxidation and protect the electronic properties against corrosion due to moisture.[22−24] The H-Si(111) surface has been alkylated with Grignard reagents to produce functionalized Si surfaces of high perfection that exhibit correspondingly low densities of electronic defects.[25−28] Similarly, a two-step halogenation/alkylation procedure has recently been used to create chemically bonded hydrocarbon monolayers on the Ge(111) surface.[29,30] Methylation of the Ge(111) surface has the capability to form a complete monolayer, because the Ge lattice spacing is sufficiently large that the van der Waals radii of the methyl groups do not

Received: June 14, 2015
Revised: July 6, 2015
Published: July 31, 2015

DOI: 10.1021/acs.jpcc.5b05678
J. Phys. Chem. C 2015, 119, 18458−18466

overlap extensively, resulting in a well-ordered, air-stable interface.

We describe herein a combined experimental and theoretical study of the atomic surface structure of CH_3-Ge(111). This work represents an extension of our previous studies of the structure and phonon dynamics of CH_3-Si(111) to the Ge system.[31−34] High-resolution helium atom scattering (HAS) and density functional theory (DFT) have been used to assess the surface structure, the effects of methyl termination on the Ge(111) bilayer spacings and step heights, and the extent of rotation of methyl groups on the (1 × 1) surface. Low-energy neutral helium atom scattering provides a nondestructive, atomic probe of structure and low-energy vibrations, with complete surface sensitivity. As will be shown herein, the methyl packing, in-plane lattice constant, and average domain size have been determined by analysis of helium diffraction patterns, including in- and out-of-phase scattering with respect to the surface normal. Because of its extremely high sensitivity to defects and exclusive surface sensitivity, a precise application of helium scattering exploiting Bragg and anti-Bragg diffraction conditions has allowed for the quantification of the CH_3-Ge(111) surface step height. Density functional theory was applied to calculate the lattice parameters, bond lengths, and bilayer spacings of CH_3-Ge(111), indicating first- and second-interlayer spacings slightly contracted from bulk values. The theoretical approach was validated with the H-Ge(111) surface, showing significant bilayer contractions, in agreement with other previously reported experimental and theoretical results. As an additional test of our slab model, the high-energy molecular vibrational modes were calculated and showed consistency with experimental FTIR and HREELS peak assignments. The rotational dynamics of the methyl group on the fully methylated Ge(111) surface were also investigated with DFT and MD simulations. DFT suggests that the rotational barrier is sufficient to hinder the free rotation of methyl groups for a fixed surface, whereas MD simulations allowing for motion of neighboring methyl groups exhibit full rotations for some methyl groups on the picosecond time scale at room temperature.

2. MATERIALS AND METHODS

2.1. Methyl-Ge(111) Sample Preparation. Unless otherwise noted, chemicals were obtained from Sigma-Aldrich or Fisher Scientific and were used as received. Water was obtained from a Barnstead E-Pure water purification system and had a resistivity of 18.2 MΩ·cm. 10% HF(aq) solutions were prepared by diluting 48 wt % HF (Transene); 3.0 M methylmagnesium chloride was purchased from Fisher Scientific and was used without further purification.

For scattering experiments, double-side polished, undoped Ge wafers (El-Cat Inc.) oriented within ±0.1° of the (111) crystal plane were cut to the desired size using a diamond scribe. The samples had a resistivity > 30 Ω·cm. Immediately prior to surface modification, the samples were cleaned by rinsing sequentially with water, methanol, acetone, methanol, and water, followed by 5 min sonication in acetone and 5 min sonication in methanol. The samples were then repeatedly dipped in 10% HF(aq) for 1 min and in 30% H_2O_2(aq) for 1 min, with a water rinse between steps. After 3 cycles of etching and oxidation, the samples were dipped in 10% HF (aq) for 1 min (a final time), rinsed with water, and dried under a stream of Ar. Cleaned Ge samples were loaded into a tube furnace that was repeatedly purged with He and pumped out before being pumped down to <0.5 mTorr. Hydrogen termination of Ge surfaces was achieved by annealing the samples at 850 °C for 15 min under 1 atm of H_2 at a flow rate of 500 sccm. The samples were cooled to <100 °C under H_2 and were immediately transferred into a N_2-purged flushbox upon removal from the tube furnace.

H-terminated Ge(111) surfaces were loaded into a N_2 purged flushbox, rinsed with anhydrous tetrahydrofuran (THF), and then methylated in 3.0 M CH_3MgCl for 59.5 h at 50 °C. Methylated surfaces were then rinsed thoroughly with anhydrous THF; removed from the N_2-purged flushbox; sequentially sonicated for 10 min in THF, methanol, and water; and dried under a stream of Ar. For transport from Pasadena, CA, to Chicago, IL, to minimize sample degradation, the samples were shipped under high vacuum in a sealed container.

2.2. Helium Scattering Instrumentation. An ultra-high vacuum (UHV) helium atom scattering apparatus with high energy and angular resolution was employed to measure the structure of methylated-Ge(111). The apparatus has been described previously.[35] The apparatus consists of three regions: a differentially pumped beam source, a UHV sample chamber, and a rotatable detector arm with a total flight path of 1.5230 m (chopper-to-crystal distance of 0.4996 m, crystal-to-ionizer distance of 1.0234 m).

Helium was expanded through a 15 μm nozzle source, which was cooled by a closed-cycle helium refrigerator, to generate a nearly monochromatic ($\Delta v/v \leq 1\%$, fwhm) supersonic neutral helium beam. A mechanical chopper modulated the helium beam in the first differentially pumped region of the beamline with a 50% duty cycle. The beam was collimated into a 4 mm spot on the crystal surface, which was housed in the UHV surface-scattering chamber (base pressure 3×10^{-10} Torr). The CH_3-Ge(111) crystals were mounted onto a six-axis manipulator that could be positioned precisely to control the incident angle, θ_i, the azimuthal angle, ϕ, and the tilt, χ, with respect to the scattering plane. Sample temperatures ranging from 30 to 900 K were achieved using a button heater and a second closed-cycle helium refrigerator. Reflected atoms entered a triply differentially pumped rotatable detector arm, were ionized via electron bombardment, and then were filtered using a quadrupole mass spectrometer.

The beam energies in these experiments ranged from 17 to 67 meV (incident wave vector, k_i = 5.7−11.3 Å^{-1}), and the surface temperatures generally ranged from 140 to 200 K. At the start of each set of experiments, the sample was first flashed to 650 K to remove trace adsorbates from the surface and then quenched to the sample temperature that was used during data acquisition. Previous work has demonstrated that similar methyl surface moieties are stable at these temperatures; the stability of the surfaces investigated was confirmed by highly sensitive helium reflectivity measurements as described herein. Diffraction patterns were recorded by aligning the crystal at a given incident angle, θ_i, and then using a computer-controlled motor to scan the detector through the final angle, θ_f.

2.3. Density Functional Theory Computational Details. The structural properties of the H-Ge(111) and CH_3-Ge(111) surfaces were calculated using density functional theory, as implemented in the QUANTUM-ESPRESSO package[36] using a norm-conserving pseudopotential for Ge and ultrasoft pseudopotentials[37] for C and H. Both the local-density approximation[38] (LDA) and the generalized gradient Perdew−Burke−Ernzerhof approximation[39] (PBE) for the

DOI: 10.1021/acs.jpcc.5b05678
J. Phys. Chem. C 2015, 119, 18458−18466

exchange-correlation energy functional were used. The electronic wave functions were expanded in plane waves up to a 28 Ry energy cutoff and a 280 Ry charge density cutoff. We optimized the bulk geometry by integrating the Brillouin zone over a 6 × 6 × 6 Monkhorst−Pack mesh.[40] The resulting equilibrium lattice parameters were a = 5.62 Å for the LDA and a = 5.77 Å for PBE, in good agreement with an experimental value of a = 5.657 Å.[41] The surface was modeled with a slab geometry and periodic boundary conditions (PBC); the slabs were composed of 18 germanium atom layers with methyl groups adsorbed on both sides, which were separated by a 12 Å wide vacuum gap. The surface Brillouin zone (SBZ) was sampled over a Monkhorst−Pack grid of 6 × 6 × 1 k-points.[40] Atomic positions were relaxed until the forces were below a 5 × 10^{-5} a.u. threshold. The vibrational frequencies at the Γ-point were calculated by diagonalizing the dynamical matrix calculated within the density functional perturbation theory (DFPT).[42]

To analyze the motion of the methyl groups at room temperature, in particular, to verify the possibility of a free rotation, *ab initio* Born−Oppenheimer molecular dynamics calculations were performed in an NVE ensemble with an average temperature of 300 K using the CP2K suite of programs[43] with a time step of 1.5 fs. In CP2K simulations, Kohn−Sham (KS) orbitals were expanded on a triple-ζ-valence plus polarization (TZVP) Gaussian-type basis set, while the charge density was expanded in a plane-wave basis set with a cutoff of 240 Ry, to efficiently solve the Poisson equation within periodic boundary conditions using the Quickstep scheme.[43] Brillouin zone integration was restricted to the 4 × 4 and 5 × 5 supercell Γ-point. CP2K simulations were performed only with the PBE functional and using Godecker−Teter−Hutter (GTH) pseudopotentials.[44,45]

3. RESULTS AND DISCUSSION

3.1. Helium Diffraction. Figure 1 shows diffraction scans taken for CH_3-Ge(111) aligned on both the ⟨$\bar{1}2\bar{1}$⟩ (black) and ⟨$01\bar{1}$⟩ (red) azimuthal directions, vertically offset for clarity. These angular distributions are plots of the reflected helium intensity as a function of the surface parallel momentum transfer, ΔK. Both distributions were taken with the same incident beam energy, E_i = 44 meV (k_i = 9.2 $Å^{-1}$), and crystal temperature, T_s = 140 K. The arrangement of the diffraction peaks is given by the periodicity of the surface, so knowledge of the azimuthal symmetry and the spacings of the diffraction peaks allows for the determination of the surface unit cell parameters. Elastic diffraction peaks arise when the kinematic condition for Bragg diffraction for in-plane scattering is met, as given by

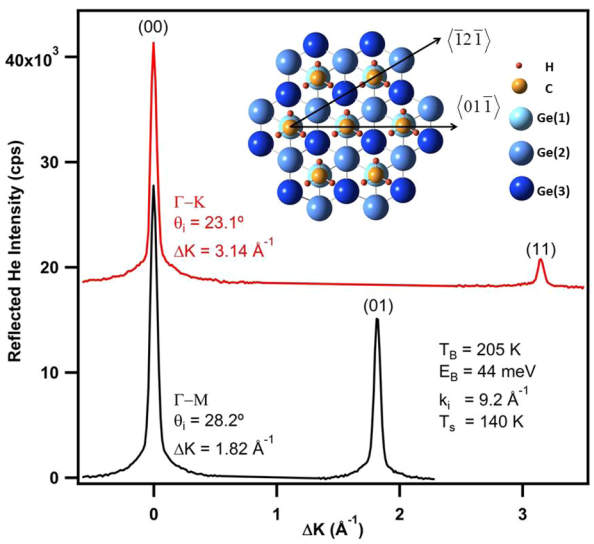

Figure 1. Helium diffraction scans for the CH_3-Ge(111) surface showing specular and first-order diffraction peaks along the ⟨$01\bar{1}$⟩ (top) and ⟨$\bar{1}2\bar{1}$⟩ (bottom) azimuths (traces vertically offset for clarity); inset displays a top view of CH_3-Ge(111) surface labeled with corresponding azimuthal orientations.

$$\Delta\vec{K} = \vec{K}_f - \vec{K}_i = \vec{k}_f \sin\theta_f - \vec{k}_i \sin\theta_i = \vec{G}_{mn} \tag{1}$$

where

$$\vec{G}_{mn} = m\vec{b}_1 + n\vec{b}_2 \tag{2}$$

and

$$\vec{b}_1 = 2\pi\frac{\vec{a}_2 \times \hat{z}}{\vec{a}_1\cdot(\vec{a}_2 \times \hat{z})} \tag{3}$$

where $\vec{K}_f$ and $\vec{K}_i$ are the surface parallel components of the helium wavevectors, θ_i and θ_f are the initial and final scattering angles, $\vec{G}_{mn}$ is the surface reciprocal lattice vector, m and n are the diffraction indices, $\vec{b}_1$ and $\vec{b}_2$ are the reciprocal lattice vectors, $\vec{a}_1$ and $\vec{a}_2$ are the primitive real space lattice vectors, and $\hat{z}$ is the surface normal unit vector. The spacings between specular (ΔK = 0 $Å^{-1}$) and the first-order diffraction peaks observed at ΔK = 1.82 $Å^{-1}$ and 3.14 $Å^{-1}$ for the ⟨$\bar{1}2\bar{1}$⟩ and ⟨$01\bar{1}$⟩ alignments, respectively, correspond to a real space lattice constant of 4.00 ± 0.02 Å for the hexagonal close-packed arrangement of the CH_3-Ge(111) surface. This value is in excellent agreement with the known spacing (4.00 Å) for the native Ge(111) surface;[46] hence, the data are fully consistent with the formation of a (1 × 1) commensurate monolayer of methyl groups on the Ge(111) surface, as visualized in the inset of Figure 1.

To a first approximation, the helium beam is scattered coherently within domains of length l_c; this coherence length is the approximate size of the atomically flat terraces of CH_3-Ge(111), separated by domain boundaries or other structural defects. The widths of the helium diffraction peaks are used to obtain the coherence length of CH_3-Ge(111), with narrower diffraction peaks corresponding to larger domain sizes. It has been shown previously[47] that the measured specular width, $\Delta\theta_{exp}$, is a convolution of the instrument function broadening, $\Delta\theta_{inst}$, and the domain size broadening, $\Delta\theta_w$. The measured broadening, therefore, allows measurement of the domain size using

$$\Delta\theta_{exp}^2 = \Delta\theta_w^2 + \Delta\theta_{inst}^2 \tag{4}$$

$$l_c = \frac{5.54}{\Delta\theta_w k_i \cos\theta_f} \tag{5}$$

The coherence length measurements were taken in-phase, with a low beam energy of ∼16.5 meV to minimize the diffuse elastic and surface defect contributions (see below) to the line width. High resolution was obtained using a crystal-to-ionizer distance of 1.0234 m, allowing for a narrow acceptance angle of 0.29° (∼0.02 $Å^{-1}$) and measurements of domain sizes up to ∼900 Å. The average measured width of the specular peaks,

DOI: 10.1021/acs.jpcc.5b05678
J. Phys. Chem. C 2015, 119, 18458−18466

fwhm = 0.46°, provides a coherence length of ∼170 Å for CH_3-Ge(111); thus, the average domain spans over nearly 50 methyl groups in a given direction. The mean terrace size of CH_3-Ge(111) is half of what has been measured in prior work for an analogous surface, CH_3-Si(111), which is consistent with the lower helium reflectivity for CH_3-Ge(111) relative to CH_3-Si(111).[31]

Normalized helium diffraction spectra taken from both CH_3-Ge(111) and CH_3-Si(111) are shown in Figure 2. The larger

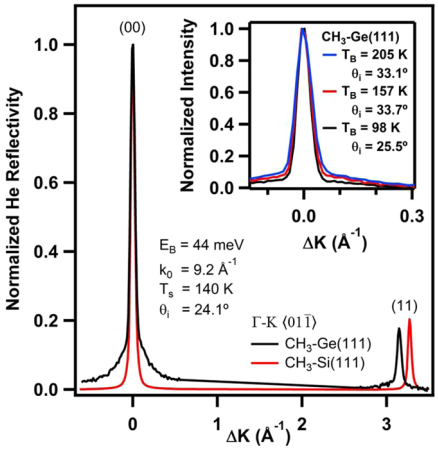

Figure 2. Comparison of helium diffraction data on CH_3-Ge(111) (black) and CH_3-Si(111) (red) along the ⟨$\bar{1}2\bar{1}$⟩ azimuth; inset demonstrates diminishing phonon contribution to "wings" of the same in-phase specular diffraction peak of CH_3-Ge(111) as a function of decreasing beam energy.

ΔK spacing observed in the CH_3-Si(111) diffraction pattern is a function of its smaller real space lattice constant (3.82 Å). The relative intensities between the specular and the first-order diffraction peaks are similar for the CH_3-Ge(111) and CH_3-Si(111) surfaces. These low-energy helium scattering potentials are directly related to the surface electron densities,[48] which we expect to be similar for two semiconductor crystals terminated with the same commensurate methyl layer. One notable difference between the two diffraction patterns was the appearance of broad shoulders, or "wings", on the CH_3-Ge(111) specular diffraction peak; this broadening of the diffraction profile provides information on how defects decorate the CH_3-Ge(111) surface.

Surface imperfections such as point defects, steps, domains, facets, and superstructures produce characteristic modifications to the elastic intensity and can, therefore, be qualitatively identified by visual inspection of the helium diffraction spectra. These static defects cause deviations from the ideal diffraction pattern to include splitting or broadening of peaks, streaks, or background.[49] Not all intensity is scattered elastically; excitations of phonons, plasmons, or electronic band transitions are all considered dynamic defects. Phonons have been shown to play a major role in the scattering and vibrational dynamics of methylated semiconductor surfaces,[33] and an extensive characterization of phonons spanning the surface Brillouin zone for CH_3-Ge(111) will be discussed separately.[50] Multiphonon scattering causes the uniform background while single-phonon excitations contribute significantly to the wings of the specular peak.[51,52] The broadening due to phonon excitations is dependent on energy, and this contribution can be reduced by lowering the incident beam energy used for CH_3-Ge(111) diffraction (Figure 2, inset). However, the intensity decay and narrowing of the diffraction line shape is not strictly a monotonic function of decreasing beam energy, but instead shows characteristic oscillations that are only possible for stepped structures.[53] Unlike regular step arrays, randomly distributed steps do not cause diffraction peak splitting; instead, they only cause peak broadening around a sharp central spike, consistent with the behavior observed herein.[54,55] By exploiting the kinematic conditions, which include the beam energy and scattering angles, the role of randomly distributed steps on the surface can be investigated further via coherent and incoherent scattering from terraces at differing heights.

The stepped nature of the surface was surveyed by scattering under both in-phase (Bragg) and out-of-phase (anti-Bragg) helium diffraction conditions. Helium atoms are not able to penetrate the surface and scatter from bulk layers; differences in their path lengths arise due to the presence of steps on the surface. The in-phase diffraction conditions correspond to constructive interference of the de Broglie waves of helium atoms specularly scattered from adjacent terraces, separated by steps, satisfying

$$k_i h(\cos\theta_i + \cos\theta_f) = 2k_i h\cos\theta_i = 2n\pi \tag{6}$$

where h is the step height and n is an integer value. Similarly, the out-of-phase conditions

$$k_i h(\cos\theta_i + \cos\theta_f) = 2k_i h\cos\theta_i = (2n+1)\pi \tag{7}$$

correspond to destructive interference between helium atoms. With known scattering conditions, these expressions allow for a unique determination of the step height of the CH_3-Ge(111) surface.

Figure 3, panel (a), shows three examples of our drift spectra, which show the relative intensity of a specularly scattered helium beam as a function of the surface-perpendicular component of the incident wavevector, $k_{perpendicular}$. Specifically, the specular intensity was monitored at three different incident angles while the temperature of the beam nozzle source was allowed to slowly drift from room temperature to 100 K over the course of ∼1 h. These runs were also repeated while undergoing a controlled drift from 100 K up to room temperature, and no significant difference was observed between the two data sets. The temperature reading from a diode attached directly to the nozzle source was calibrated against the actual helium beam energy by use of a series of time-of-flight runs over the range of nozzle temperatures.

Peaks and dips in the drift spectra arise from coherent and incoherent scattering accessed by varying the beam energy, or the incident angle (Figure 3b), of the incoming helium atoms. The peak maxima and minima in our drift spectra (Figure 3a) correspond to the different in- (n) and out-of-phase (n + 0.5) scattering conditions, respectively. Figure 3c shows diffraction spectra for the n =7 and n = 7.5 conditions. The drift spectra taken at three different incident angles exhibited the same k_{perp} peak maxima and minima, within experimental error. The baselines of the scattered intensities have been normalized to account for changes associated with Debye−Waller effects and a changing helium beam flux over the temperature range of data collection. The step height was extracted from each peak maximum and minimum, and these values were then averaged. The experimental data yield a calculated step height of 3.28 ± 0.02 Å. This value, within the precision of these measurements, is equivalent to the (111) interlayer spacing of 3.27 Å known

DOI: 10.1021/acs.jpcc.5b05678
J. Phys. Chem. C 2015, 119, 18458−18466

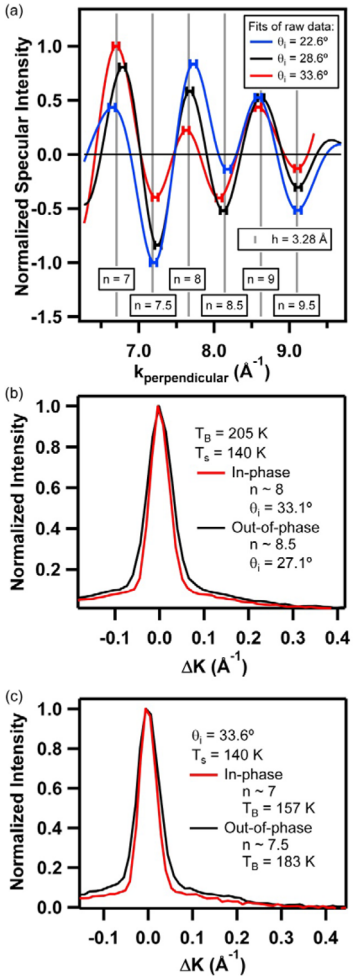

Figure 3. (a) Multipeak fits to specularly scattered drift spectra at three different incident angles, normalized for comparison, with error bars arising from slight experimental uncertainty in beam temperature; vertical lines represent expected positions of peak maxima and minima as determined from eqs 6 and 7 for de Broglie wavelength interference for a step height of 3.28 Å. Below: comparison of in- and out-of-phase specular diffraction peaks by varying (b) beam temperature and (c) incident angle.

for the ideal, unrelaxed diamond-lattice configuration of Ge(111).[9,12] Electronic structure calculations reported herein are in agreement with this experimentally measured CH_3-Ge(111) step height and will be used to provide further insight into substrate relaxations not extractable from scattering measurements.

3.2. Model Calculations. To complement our scattering results, a slab model of the (1 × 1) methyl-terminated Ge(111) interface was generated and investigated using density functional theory. Two approximations were used to calculate the crystal structure, with the equilibrium lattice parameters a = 5.62 Å for the LDA and a = 5.77 Å for the PBE approximation. In the optimized CH_3-Ge(111) structure, the calculated bond lengths for C−H and C−Ge were 1.102 and 1.974 Å, respectively, for the LDA functional (surface lattice constant = 3.972 Å) while 1.098 and 2.008 Å were obtained within the PBE approximation (surface lattice constant = 4.076 Å). Additionally, the dihedral angle for H−C−Ge−Ge, which defines the rotation of the surface methyl groups about the Ge−C axis, was found to be 41.9° (LDA) and 41.3° (PBE), both of which are slightly larger than the value of 37.7° calculated for the analogous CH_3-Si(111) surface.[49,56] In addition to the crystal lattice constants and adlayer bond lengths, additional structural parameters, such as the Ge−Ge bilayer spacings, which play a major role in the interfacial charge density, have also been calculated. The first (d_{12}) and second (d_{23}) Ge bilayer spacings sum together to produce the surface step height ($d_{step} = d_{12} + d_{23}$), as visualized in Figure 4, and also measured via helium scattering.

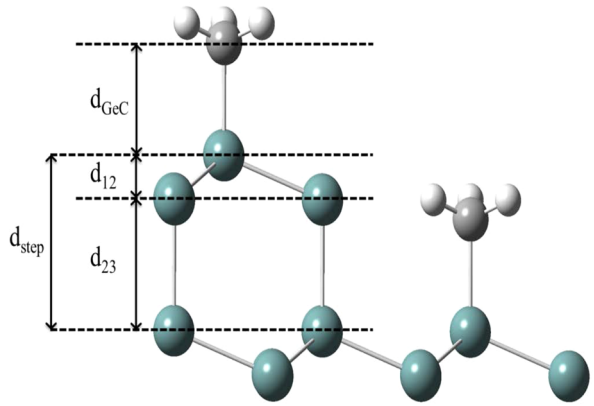

Figure 4. Lateral view of the CH_3-Ge(111) lattice exhibiting a single step along the $\langle \bar{1}2\bar{1} \rangle$ orientation; d_{12} and d_{23} define the first and second bilayer spacings, respectively.

As an initial test of our CH_3-Ge(111) slab surface, the molecular vibrational modes of the adsorbed methyl groups were calculated using density functional perturbation theory at the Γ-point. The frequencies of the six high-energy molecular modes, including the methyl stretching, deformation, and rocking, are presented in Table 1, via both the LDA and the PBE approximation. The calculated frequencies are compared with experimentally observed peaks from Wong et al.[57] as measured using Fourier transform infrared spectroscopy (FTIR) and high-resolution electron energy loss spectroscopy (HREELS). Overall, the consistency observed between our calculated frequencies and both the FTIR and the HREELS data provide further validation of our model of the CH_3-Ge(111) interface.

The effects of an adlayer, such as hydrogen, on the atomic structure and spacings of Ge and Si semiconductors have been observed with both experiment and theory.[7−14] We report herein the first investigation into the structural changes of the Ge(111) interface due to methyl termination. As a consistency check, the model and calculations have also been applied to H-Ge(111)-(1 × 1). Table 2 shows the first and second bilayer spacings, along with the Ge−H bond length. A significant inward contraction of d_{12} was obtained, which agrees with theory[9,13] and experiment.[12] A smaller inward contraction was obtained for d_{23} relative to ideal Ge(111) bulk values. Inward relaxations are commonly found on the outermost layers of bare surfaces, whereas hydrogen would be expected to saturate the dangling bonds and remove this relaxation. Instead, the contraction of the bilayer spacing has been explained by Kaxiras and Joannopoulos,[9] who argue that an electronegativity difference between Ge and H induces a dipole moment, which would be partially canceled by a charge transfer from the Ge−H bond into the Ge−Ge back-bond. This charge transfer would strengthen and shorten the back-bond, causing the outer

DOI: 10.1021/acs.jpcc.5b05678
J. Phys. Chem. C 2015, 119, 18458−18466

Table 1. Frequencies (cm^{-1}) at the Γ-Point for the High-Energy Modes of CH_3-Ge(111)

mode	PBE	LDA	transmission FTIR[a]	HREELS[a]
M1 (CH_3 asymmetric stretch)	3052	3030	2928, 2906	2910[b]
M2 (CH_3 symmetric stretch)	2956	2923	2956, 2860	2910[b]
M3 (CH_3 asymmetric deformation)	1404	1366	[c]	1411
M4 (CH_3 symmetric deformation)	1200	1187	1234	1234
M5 (CH_3 internal rocking)	731	739	762	780
M6 (Ge−C stretch)	530	557	[d]	568

[a]Reference 57. [b]Symmetric and asymmetric C−H stretches unresolved by HREELS. [c]Not IR-active. [d]Not visible above noise.

Table 2. Structural Parameters of Terminated Ge(111) Using the PBE and LDA Approximations

	PBE			LDA		
	ideal bulk	H−	CH_3−	ideal bulk	H−	CH_3−
lattice parameter		4.0764			3.97245	
d_{Ge-H} (d_{Ge-C})		1.56211	2.00879		1.54231	1.97400
d_{12}	0.82925	0.78689	0.81547	0.80947	0.76918	0.79141
$\Delta d_{12}/d_{bulk}$		−5.10%	−1.66%		−4.97%	−2.23%
d_{23}	2.49917	2.48423	2.48410	2.43403	2.42157	2.42158
$\Delta d_{23}/d_{bulk}$		−0.60%	−0.60%		−0.52%	−0.51%

Ge layer to contract toward the bulk. As a result of the inward contraction of both the first and the second bilayer, the calculations indicate an overall contraction of 0.057 Å (PBE) and 0.053 Å (LDA) in the H-Ge(111) step height from a bulk value of 3.328 Å. These results are in excellent agreement with previous quantitative low-energy electron diffraction results which determined an overall step height contraction of 0.05 Å due to the hydrogen termination of the Ge(111) surface.[12]

Having successfully modeled the H-Ge(111) interface, the structural effects of terminating the Ge(111) surface with methyl groups were then investigated. Table 2 lists the lattice parameters, Ge−C bond lengths, and bilayer spacings for the ideal bulk and methyl-terminated Ge(111), respectively, using the PBE and LDA approximations. The interlayer spacings of the ideal truncated bulk Ge(111) result in a step height of 3.244 Å (LDA) and 3.328 Å (PBE); the experimental value of 3.28 Å reported above lies between these two values, demonstrating agreement with the modeled surface. An inward contraction of the first and second Ge bilayers due to functionalization is obtained from the calculations for CH_3-Ge(111); the magnitude of the contraction for the first Ge bilayer was 2.23% (LDA) and 1.66% (PBE), with respect to the ideal truncated bulk values. The second bilayer was calculated to contract 0.51% (LDA) and 0.60% (PBE), which is nearly identical to what was calculated for H-Ge(111). These first and second bilayer contractions, relative to H-Ge(111), suggest minimal electronic charge transfer between the outermost Ge atoms and the adsorbed methyl groups.

The rotational character of the methyl groups on the Ge(111) surface was investigated to investigate whether the surface methyl groups were locked, hindered, or freely rotating. The rotational barrier was calculated by employing a 2 × 2 supercell with the same slab configuration used for the structural properties, but with a 3 × 3 × 1 *k*-point sampling. Two extreme cases were considered: (a) a fully methylated surface in which only one methyl group was rotated and the position of the neighboring groups was fixed, and (b) an isolated methyl group on an otherwise hydrogen-terminated Ge(111) surface. These approximations can provide both upper and lower boundaries for the rotational barrier of the real system, wherein all of the methyl groups are free to rearrange to compensate for the steric interactions due to rotations of neighboring methyl groups.

Figure 5 shows the energy profiles of both rotational barriers as a function of the methyl rotation angle with respect to its equilibrium position. The rotational activation barrier for the methylated Ge(111) surface with fixed neighbors was calculated to be ∼55 meV, with the highest energy measured at a 60° rotation from equilibrium. Sum frequency generation (SFG) experiments[58] and DFT calculations[34] proposed a hindered rotation of the analogous methylated Si(111) surface, with Brown et al.[34] calculating a rotational barrier of 112 meV, arising predominately from the close packing of neighboring methyl groups. The helium diffraction data described above indicate that the methyl spacing for CH_3-Ge(111) is larger than that for CH_3-Si(111), which is consistent with a significant lowering of the calculated rotational activation barrier from 112 meV for CH_3-Si(111) to 55 meV for CH_3-Ge(111). Even with a larger lattice spacing, the steric interactions from neighboring

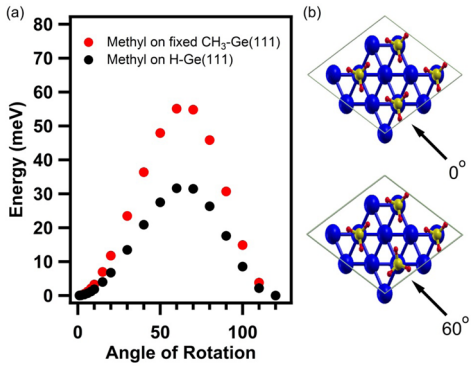

Figure 5. (a) The change in potential energy as a function of the rotation of a surface methyl group from its equilibrium conformation, for a rotationally fixed methylated Ge(111) surface (red) and an isolated methyl group residing on a H-Ge(111) surface (black), calculated using the PBE approximation for the exchange-correlation functional. (b) Top view of CH_3-Ge(111) showing the surface methyl group in its equilibrium rotational conformation (top) and highest-energy rotational conformation (bottom).

DOI: 10.1021/acs.jpcc.5b05678
J. Phys. Chem. C 2015, 119, 18458−18466

methyl groups on CH_3-Ge(111) still play a role in the rotational barrier. By replacing the neighboring methyl groups with hydrogens, the rotational barrier decreased further, from 55 to 32 meV. The lower-bound activation barrier of 32 meV for an isolated methyl group surrounded by H-Ge(111) presents a notable corrugation in the rotational potential for this model system as compared to kT (25.7 meV at room temperature). These DFT calculations, therefore, suggest that the free rotation of the methyl groups on the CH_3-Ge(111) surface is hindered at room temperature.

As mentioned above, concerted motion of neighboring methyl groups might bring the rotational barrier closer to the lower bound given by the model system specified by an isolated methyl group on a hydrogen-terminated Ge(111) surface. To investigate this possibility, DFT molecular dynamics (MD) simulations were performed using the CP2k suite of programs.[43] Two slab models were considered, with a 4 × 4 or 5 × 5 surface supercell that contained, respectively, 16 or 25 methyl groups grafted on both surfaces of a 6-layer slab of Ge. After equilibration at 300 K, the rotational dynamics were analyzed over a 1.3 ps interval. Figure 6 shows snapshots of the largest model in the initial (ordered) and final configurations. In the larger model, 5 methyl groups out of 25 underwent one or several (up to five) complete rotations in 1.3 ps. These results suggest that, although most methyl groups undergo hindered rotation, cooperative motion allows for some methyl groups to perform complete rotations on the picosecond time scale at room temperature.

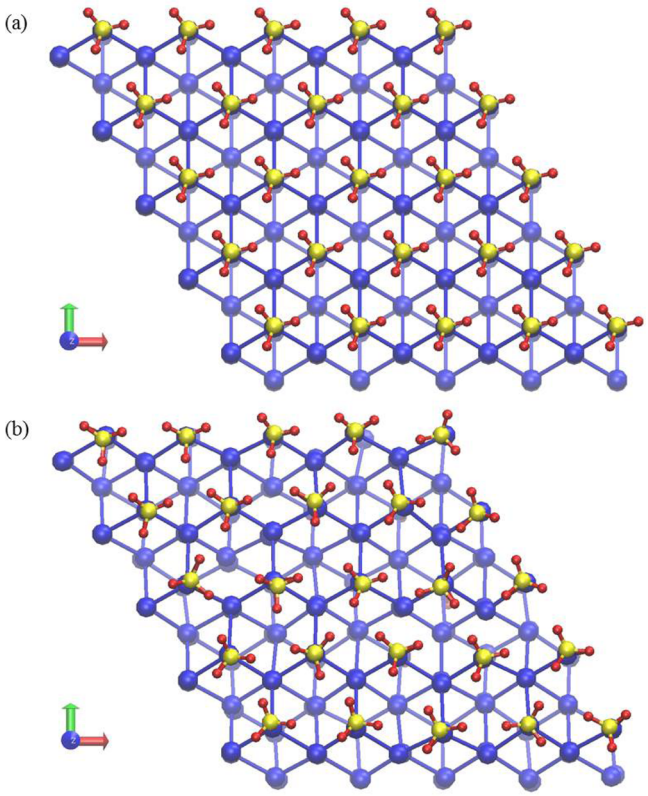

Figure 6. Snapshots of the 5 × 5 surface supercell (a) before and (b) after a molecular dynamics simulation 1.3 ps long at 300 K. Five methyl groups out of 25 undergo one or more complete rotations due to the cooperative motion of the neighboring CH_3 groups.

4. CONCLUSIONS

A combined experimental/theoretical approach using low-energy helium diffraction data and density functional theory has been used to characterize the atomic surface structure of methyl-terminated Ge(111). Helium diffraction patterns for two primary azimuths showed that methyl termination of the Ge(111) surface creates a (1 × 1) hexagonally packed adlayer, preserving the native, unreconstructed structure of the Ge(111) crystal. The diffraction peaks indicated the presence of large domains of CH_3-Ge(111), while also revealing the presence of atomic steps. Drift spectra, which measure diffraction intensity as a function of the helium perpendicular wavevector, utilize data obtained under Bragg and anti-Bragg scattering conditions to experimentally determine the surface step height. Density functional theory yielded an optimized structure of CH_3-Ge(111). Bulk spacings were in quantitative agreement with the step height measured from scattering, and organic functionalization of the surface resulted in small inward relaxations of the first and second Ge(111) bilayers with respect to bulk Ge(111). The close proximity of neighboring methyl groups results in a rotational activation barrier that is sufficient to hinder the free rotation of methyl groups on the fixed CH_3-Ge(111) surface at room temperature. However, cooperative motion of neighboring methyl groups allows for few of the methyl groups to undergo complete rotations on a picosecond time scale. Hence, a detailed investigation of this hybrid organic−semiconductor surface, using scattering and calculations, has revealed the effects of methylation on the atomic structure, interlayer spacings, and rotational character of the methyl groups decorating Ge(111).

■ AUTHOR INFORMATION

Corresponding Author

*E-mail: s-sibener@uchicago.edu. Tel.: 773-702-7193.

Notes

The authors declare no competing financial interest.

■ ACKNOWLEDGMENTS

S.J.S. acknowledges support from the Air Force Office of Scientific Research Grant No. FA9550-10-1-0219, and the Material Research Science and Engineering Center at the University of Chicago, NSF-DMR-14-20709. N.S.L. acknowledges support from the National Science Foundation (CHE-1214152), and the research was in part carried out at the Molecular Materials Research Center of the Beckman Institute of the California Institute of Technology.

■ REFERENCES

(1) Frank, M. M.; Koester, S. J.; Copel, M.; Ott, J. A.; Paruchuri, V. K.; Shang, H.; Loesing, R. Hafnium Oxide Gate Dielectrics on Sulfur-Passivated Germanium. *Appl. Phys. Lett.* **2006**, *89*, 112905.

(2) Brunco, D. P.; De Jaeger, B.; Eneman, G.; Mitard, J.; Hellings, G.; Satta, A.; Terzieva, V.; Souriau, L.; Leys, F. E.; Pourtois, G.; et al. Germanium MOSFET Devices: Advances in Materials Understanding, Process Development, and Electrical Performance. *J. Electrochem. Soc.* **2008**, *155*, H552.

(3) Guter, W.; Schöne, J.; Philipps, S. P.; Steiner, M.; Siefer, G.; Wekkeli, A.; Welser, E.; Oliva, E.; Bett, A. W.; Dimroth, F. Current-Matched Triple-Junction Solar Cell Reaching 41.1% Conversion Efficiency under Concentrated Sunlight. *Appl. Phys. Lett.* **2009**, *94*, 223504.

(4) King, R. R.; Law, D. C.; Edmondson, K. M.; Fetzer, C. M.; Kinsey, G. S.; Yoon, H.; Sherif, R. A.; Karam, N. H. 40% Efficient

Metamorphic GaInP/GaInAs/Ge Multijunction Solar Cells. *Appl. Phys. Lett.* **2007**, *90*, 183516.
(5) Montgomery, H. C.; Brown, W. L. Field-Induced Conductivity Changes in Germanium. *Phys. Rev.* **1956**, *103*, 865−870.
(6) Kingston, R. H. Water-Vapor-Induced n-Type Surface Conductivity on p-Type Germanium. *Phys. Rev.* **1955**, *98*, 1766−1775.
(7) Jona, F.; Thompson, W. A.; Marcus, P. M. Experimental Determination of the Atomic Structure of a H-Terminated Si{111} Surface. *Phys. Rev. B: Condens. Matter Mater. Phys.* **1995**, *52*, 8226−8230.
(8) Cargnoni, F.; Gatti, C.; May, E.; Narducci, D. Geometrical Reconstructions and Electronic Relaxations of Silicon Surfaces. I. An Electron Density Topological Study of H-Covered and Clean Si(111) (1 × 1) Surfaces. *J. Chem. Phys.* **2000**, *112*, 887−899.
(9) Kaxiras, E.; Joannopoulos, J. D. Hydrogenation of Semiconductor Surfaces: Si and Ge (111). *Phys. Rev. B: Condens. Matter Mater. Phys.* **1988**, *37*, 8842−8848.
(10) Li, X.-P.; Vanderbilt, D.; King-Smith, R. D. First-Principles Study of Steps on the Si(111):H Surface. *Phys. Rev. B: Condens. Matter Mater. Phys.* **1994**, *50*, 4637−4641.
(11) Stumpf, R.; Marcus, P. M. Relaxation of the Clean and H-Covered C(111) and the Clean Si(111)-1 × 1 Surfaces. *Phys. Rev. B: Condens. Matter Mater. Phys.* **1993**, *47*, 16016−16019.
(12) Imbihl, R.; Demuth, J. E.; Himpsel, F. J.; Marcus, P. M.; Thompson, W. A.; Jona, F. Structure Analysis of Ge(111)1 × 1-H by Low-Energy Electron Diffraction. *Phys. Rev. B: Condens. Matter Mater. Phys.* **1987**, *36*, 5037−5040.
(13) Ong, C. K. The Relaxation of the H-Terminated Diamond (C), Si and Ge (111) Surfaces. *Solid State Commun.* **1989**, *70*, 225−227.
(14) Copel, M.; Culbertson, R. J.; Tromp, R. M. Relaxation and H Coverage of Ammonium Fluoride Treated Si(111). *Appl. Phys. Lett.* **1994**, *65*, 2344−2346.
(15) Loscutoff, P. W.; Bent, S. F. Reactivity of the Germanium Surface: Chemical Passivation and Functionalization. *Annu. Rev. Phys. Chem.* **2006**, *57*, 467−495.
(16) Rivillon, S.; Chabal, Y. J.; Amy, F.; Kahn, A. Hydrogen Passivation of Germanium (100) Surface Using Wet Chemical Preparation. *Appl. Phys. Lett.* **2005**, *87*, 253101.
(17) Linford, M. R.; Fenter, P.; Eisenberger, P. M.; Chidsey, C. E. D. Alkyl Monolayers on Silicon Prepared from 1-Alkenes and Hydrogen-Terminated Silicon. *J. Am. Chem. Soc.* **1995**, *117*, 3145−3155.
(18) Buriak, J. M. Organometallic Chemistry on Silicon and Germanium Surfaces. *Chem. Rev.* **2002**, *102*, 1271−1308.
(19) Sharp, I. D.; Schoell, S. J.; Hoeb, M.; Brandt, M. S.; Stutzmann, M. Electronic Properties of Self-Assembled Alkyl Monolayers on Ge Surfaces. *Appl. Phys. Lett.* **2008**, *92*, 223306.
(20) Gorostiza, P.; de Villeneuve, C. H.; Sun, Q. Y.; Sanz, F.; Wallart, X.; Boukherroub, R.; Allongue, P. Water Exclusion at the Nanometer Scale Provides Long-Term Passivation of Silicon (111) Grafted with Alkyl Monolayers. *J. Phys. Chem. B* **2006**, *110*, 5576−5585.
(21) Choi, K.; Buriak, J. M. Hydrogermylation of Alkenes and Alkynes on Hydride-Terminated Ge(100) Surfaces. *Langmuir* **2000**, *16*, 7737−7741.
(22) Bodlaki, D.; Yamamoto, H.; Waldeck, D. H.; Borguet, E. Ambient Stability of Chemically Passivated Germanium Interfaces. *Surf. Sci.* **2003**, *543*, 63−74.
(23) He, J.; Lu, Z.-H.; Mitchell, S. A.; Wayner, D. D. M. Self-Assembly of Alkyl Monolayers on Ge(111). *J. Am. Chem. Soc.* **1998**, *120*, 2660−2661.
(24) Cullen, G. W.; Amick, J. A.; Gerlich, D. The Stabilization of Germanium Surfaces by Ethylation. *J. Electrochem. Soc.* **1962**, *109*, 124−127.
(25) Royea, W. J.; Juang, A.; Lewis, N. S. Preparation of Air-Stable, Low Recombination Velocity Si(111) Surfaces through Alkyl Termination. *Appl. Phys. Lett.* **2000**, *77*, 1988−1990.
(26) Yu, H.; Webb, L. J.; Heath, J. R.; Lewis, N. S. Scanning Tunneling Spectroscopy of Methyl- and Ethyl-Terminated Si(111) Surfaces. *Appl. Phys. Lett.* **2006**, *88*, 252111.
(27) Bansal, A.; Li, X.; Lauermann, I.; Lewis, N. S.; Yi, S. I.; Weinberg, W. H. Alkylation of Si Surfaces Using a Two-Step Halogenation/Grignard Route. *J. Am. Chem. Soc.* **1996**, *118*, 7225−7226.
(28) Bansal, A.; Lewis, N. S. Stabilization of Si Photoanodes in Aqueous Electrolytes through Surface Alkylation. *J. Phys. Chem. B* **1998**, *102*, 4058−4060.
(29) Knapp, D.; Brunschwig, B. S.; Lewis, N. S. Chemical, Electronic, and Electrical Properties of Alkylated Ge(111) Surfaces. *J. Phys. Chem. C* **2010**, *114*, 12300−12307.
(30) Knapp, D.; Brunschwig, B.; Lewis, N. S. Transmission Infrared Spectra of CH_3−, CD_3−, and $C_{10}H_{21}$−Ge (111) Surfaces. *J. Phys. Chem. C* **2011**, *115*, 16389−16397.
(31) Becker, J. S.; Brown, R. D.; Johansson, E.; Lewis, N. S.; Sibener, S. J. Helium Atom Diffraction Measurements of the Surface Structure and Vibrational Dynamics of CH_3-Si(111) and CD_3-Si(111) Surfaces. *J. Chem. Phys.* **2010**, *133*, 104705.
(32) Brown, R. D.; Tong, Q.; Becker, J. S.; Freedman, M. A.; Yufa, N. A.; Sibener, S. J. Dynamics of Molecular and Polymeric Interfaces Probed with Atomic Beam Scattering and Scanning Probe Imaging. *Faraday Discuss.* **2012**, *157*, 307−323.
(33) Brown, R. D.; Hund, Z. M.; Campi, D.; O'Leary, L. E.; Lewis, N. S.; Bernasconi, M.; Benedek, G.; Sibener, S. J. Hybridization of Surface Waves with Organic Adlayer Librations: A Helium Atom Scattering and Density Functional Perturbation Theory Study of Methyl-Si(111). *Phys. Rev. Lett.* **2013**, *110*, 156102.
(34) Brown, R. D.; Hund, Z. M.; Campi, D.; O'Leary, L. E.; Lewis, N. S.; Bernasconi, M.; Benedek, G.; Sibener, S. J. The Interaction of Organic Adsorbate Vibrations with Substrate Lattice Waves in Methyl-Si(111)-(1 × 1). *J. Chem. Phys.* **2014**, *141*, 024702.
(35) Gans, B.; Knipp, P. A.; Koleske, D. D.; Sibener, S. J. Surface Dynamics of Ordered Cu_3Au(001) Studied by Elastic and Inelastic Helium Atom Scattering. *Surf. Sci.* **1992**, *264*, 81−94.
(36) Giannozzi, P.; Baroni, S.; Bonini, N.; Calandra, M.; Car, R.; Cavazzoni, C.; Ceresoli, D.; Chiarotti, G. L.; Cococcioni, M.; Dabo, I.; et al. QUANTUM ESPRESSO: A Modular and Open-Source Software Project for Quantum Simulations of Materials. *J. Phys.: Condens. Matter* **2009**, *21*, 395502.
(37) Vanderbilt, D. Soft Self-Consistent Pseudopotentials in a Generalized Eigenvalue Formalism. *Phys. Rev. B: Condens. Matter Mater. Phys.* **1990**, *41*, 7892−7895.
(38) Perdew, J. P.; Zunger, A. Self-Interaction Correction to Density-Functional Approximations for Many-Electron Systems. *Phys. Rev. B: Condens. Matter Mater. Phys.* **1981**, *23*, 5048−5079.
(39) Perdew, J. P.; Burke, K.; Ernzerhof, M. Generalized Gradient Approximation Made Simple. *Phys. Rev. Lett.* **1996**, *77*, 3865−3868.
(40) Monkhorst, H. J.; Pack, J. D. Special Points for Brillouin-Zone Integrations. *Phys. Rev. B* **1976**, *13*, 5188−5192.
(41) Hom, T.; Kiszenik, W.; Post, B. Accurate Lattice Constants from Multiple Reflection Measurements II. Lattice Constants of Germanium, Silicon and Diamond. *J. Appl. Crystallogr.* **1975**, *8*, 457−458.
(42) Baroni, S.; de Gironcoli, S.; Dal Corso, A.; Giannozzi, P. Phonons and Related Crystal Properties from Density-Functional Perturbation Theory. *Rev. Mod. Phys.* **2001**, *73*, 515−562.
(43) Vandevondele, J.; Krack, M.; Mohamed, F.; Parrinello, M.; Chassaing, T.; Hutter, J. QUICKSTEP: Fast and Accurate Density Functional Calculations Using a Mixed Gaussian and Plane Waves Approach. *Comput. Phys. Commun.* **2005**, *167*, 103−128.
(44) Goedecker, S.; Teter, M.; Hutter, J. Separable Dual-Space Gaussian Pseudopotentials. *Phys. Rev. B: Condens. Matter Mater. Phys.* **1996**, *54*, 1703−1710.
(45) Krack, M. Pseudopotentials for H to Kr Optimized for Gradient-Corrected Exchange-Correlation Functionals. *Theor. Chem. Acc.* **2005**, *114*, 145−152.
(46) Cao, S.; Tang, J.-C.; Shen, S.-L. Multiple-Scattering and DV-Xa Analyses of a Cl-Passivated Ge(111) Surface. *J. Phys.: Condens. Matter* **2003**, *15*, 5261−5268.

DOI: 10.1021/acs.jpcc.5b05678
J. Phys. Chem. C 2015, 119, 18458−18466

(47) Lapujoulade, J.; Lejay, Y.; Armand, G. The Thermal Attenuation of Coherent Elastic Scattering of Noble Gas from Metal Surfaces. *Surf. Sci.* **1980**, *95*, 107−130.
(48) Esbjerg, N.; Nørskov, J. K. Dependence of the He-Scattering Potential at Surfaces on the Surface-Electron-Density Profile. *Phys. Rev. Lett.* **1980**, *45*, 807−810.
(49) Henzler, M. Measurement of Surface Defects by Low-Energy Electron Diffraction. *Appl. Phys. A: Solids Surf.* **1984**, *34*, 205−214.
(50) Hund, Z. M.; Nihill, K. J.; Campi, D.; Wong, K. T.; Lewis, N. S.; Bernasconi, M.; Benedek, G.; Sibener, S. J. Vibrational Dynamics and Band Structure of CH_3-Ge(111), submitted, **2015**.
(51) Zielasek, V.; Büssenschütt, A.; Henzler, M. Low-Energy Electron Thermal Diffuse Scattering from Al(111) Individually Resolved in Energy and Momentum. *Phys. Rev. B: Condens. Matter Mater. Phys.* **1997**, *55*, 5398−5403.
(52) Barnes, R. F.; Lagally, M. G.; Webb, M. B. Multiphonon Scattering of Low-Energy Electrons. *Phys. Rev.* **1968**, *171*, 627−633.
(53) Henzler, M. LEED Studies of Surface Imperfections. *Appl. Surf. Sci.* **1982**, *11*−*12*, 450−469.
(54) Henzler, M. Quantitative Evaluation of Random Distributed Steps at Interfaces and Surfaces. *Surf. Sci.* **1978**, *73*, 240−251.
(55) Niu, L.; Gaspar, D. J.; Sibener, S. J. Phonons Localized at Step Edges: A Route to Understanding Forces at Extended Surface Defects. *Science* **1995**, *268*, 847−850.
(56) Solares, S. D.; Yu, H.; Webb, L. J.; Lewis, N. S.; Heath, J. R.; Goddard, W. A. Chlorination-Methylation of the Hydrogen-Terminated Silicon(111) Surface Can Induce a Stacking Fault in the Presence of Etch Pits. *J. Am. Chem. Soc.* **2006**, *128*, 3850−3851.
(57) Wong, K. T.; Kim, Y.-G.; Soriaga, M. P.; Brunschwig, B. S.; Lewis, N. S. Synthesis and Characterization of Atomically Flat Methyl-Terminated Ge(111). *J. Am. Chem. Soc.* **2015**, *137*, 9006−9014.
(58) Malyk, S.; Shalhout, F. Y.; O'Leary, L. E.; Lewis, N. S.; Benderskii, A. V. Vibrational Sum Frequency Spectroscopic Investigation of the Azimuthal Anisotropy and Rotational Dynamics of Methyl-Terminated Silicon(111) Surfaces. *J. Phys. Chem. C* **2013**, *117*, 935−944.

DOI: 10.1021/acs.jpcc.5b05678
J. Phys. Chem. C 2015, 119, 18458−18466